Identification of a stable phase for the high-capacity hydrogen-storage material $Zn(BH_4)_2$ from density functional theory and lattice dynamics

Pabitra Choudhury,[1,2] Venkat R. Bhethanabotla,[1,2,*] and Elias Stefanakos[2]
[1]*Sensors Research Laboratory (SRL), Department of Chemical Engineering, University of South Florida, 4202 East Fowler Avenue, Tampa, Florida 33620-5350, USA*
[2]*Clean Energy Research Center (CERC), University of South Florida, 4202 East Fowler Avenue, Tampa, Florida 33620-5350, USA*
(Received 20 July 2007; revised manuscript received 16 January 2008; published 3 April 2008)

First-principles calculations were performed on $Zn(BH_4)_2$ using density functional theory (DFT) within the local density approximation and the projected augmented wave method. $Zn(BH_4)_2$ is a promising candidate for hydrogen storage with a capacity of 8.5 wt %. A direct method lattice dynamics approach using *ab initio* force constants was utilized to calculate the phonon dispersion curves. This allowed us to establish the stability of the crystal structure at finite temperatures. DFT was used to calculate electronic properties and the direct method lattice dynamics was used to calculate the finite temperature thermal properties. $Zn(BH_4)_2$ is found to have an orthorhombic structure in the space group of $Pmc2_1$ with lattice parameters $a=4.118$ Å, $b=4.864$ Å, $c=7.916$ Å. It is an insulating material having a DFT-calculated band gap of 3.529 eV. Analysis of the electronic structure shows strong bonding between hydrogen atoms and boron in the $[BH_4]^-$ complex and also less polar bonding between the Zn and the hydrogen atom. The reaction enthalpy was calculated for the reaction $Zn(BH_4)_2=Zn+2B+4H_2(g)$ to be 76.91 kJ/mol of H_2 at 0 K without any zero point energy correction, and 59.90 kJ/mol of H_2 including the zero point energy correction. The simulated standard enthalpy of formation for the complex $Zn(BH_4)_2$ was found to be −66.003 kJ/mol of H_2 at 300 K. This suggests that the crystal structure of $Zn(BH_4)_2$ is stable at room temperature and this complex hydride can thus be considered a potential candidate for hydrogen storage.

DOI: 10.1103/PhysRevB.77.134302 PACS number(s): 61.66.−f, 63.20.D−, 65.40.G−, 71.20.−b

I. INTRODUCTION

A recent challenge in hydrogen storage is to find light weight complex solid hydrides which have higher gravimetric system capacity greater than 6.5 wt % for on-board vehicular applications. The technical challenge is to find materials that can exhibit favorable thermodynamics and kinetics for hydrogen desorption and absorption, and have the ability to store a sufficient amount of hydrogen by weight as well as by volume percent. Borohydride complexes as hydrogen storage materials have recently attracted great interest. The stabilities of borohydrides have been studied using first-principles calculations. Some researchers have reported that alkali borohydrides are too stable for hydrogen storage.[1,2] Lithium borohydride ($LiBH_4$) possesses a theoretical hydrogen capacity of ~18.3 wt %, exhibiting potential promise for on-board applications. However, hydrogen decomposition from $LiBH_4$ starts at an elevated temperature of 380 °C and, also, this compound shows little or no reversible hydrogenation behavior. It has been reported that catalytically doping with SiO_2 lowers this temperature of hydrogen evolution to 300 °C.[3] A systematic approach to study the phase stability of $LiBH_4$ based on *ab initio* calculations has been presented and four thermodynamically stable phases have been identified, including a phase of *Cc* symmetry for $LiBH_4$.[4] A correlation has been reported between thermodynamic stability of metal borohydrides and Pauli electronegativity of the parent components using first-principles calculations.[5]

Most of the commonly known borohydrides are found to be unsuitable for on-board hydrogen storage applications. This is primarily attributable to the high stability resulting from very high decomposition temperatures or complete irreversibility of hydrogen desorption.[6] $Zn(BH_4)_2$ is considered a potential candidate for on-board applications as it has a very high theoretical hydrogen storage capacity of 8.5 wt % and a reasonably low decomposition temperature (85 °C) compared to complex alkali borohydrides (greater than 300 °C).[7]

Density functional theory (DFT) is at present considered to be a versatile and important tool to solve innovative research problems in metal-hydrogen interactions and associated mechanisms. Successful application of DFT to a materials problem involves three distinct steps: (i) translation of the engineering problem to a computable atomistic model, (ii) computation of the required physicochemical properties, and (iii) validation of the simulation results by comparison with laboratory experiments.[8] Lattice dynamics[9,10] using a direct force constant method helps one complete the picture by allowing for calculation of the finite temperature thermodynamic properties. Recently, in hydrogen storage materials research, DFT calculations have been employed to understand and validate the catalytic behavior of Ti species on the dehydrogenation of $NaAlH_4$ clusters.[11–13] Crystal structure stability and electronic structure for storing high hydrogen content in light weight complex hydrides[14,15] have been reported on the basis of DFT calculations.

Although $Zn(BH_4)_2$ is a potential candidate for hydrogen storage, very little is known about its structural and thermodynamic properties. In this study, we performed *ab initio* DFT calculations to establish the 0 K crystal structure and electronic structure. We then performed lattice dynamics calculations[16] to determine the finite temperature reaction enthalpy of $Zn(BH_4)_2$. We employed the criterion that $\omega^2>0$ from the phonon frequencies to establish finite-temperature

TABLE I. Ground-state energy E in eV/mol of Zn, B, and H_2 from DFT calculations.

Element/ compound	Space group (number)/ type	E (this work) (eV/unit formula)	E (literature) (eV/unit formula)
Zn	$P63/mmc(194)/hcp$ (Refs. 26 and 27)	−0.922	−1.02
H_2	$P63/mmc(194)/hcp$ (Refs. 28 and 29)	−6.782	−6.792
α-B	R-$3m(166)$/trigonal (Refs. 30 and 31)	−6.678	−6.479

stability of the crystal structure determined from DFT calculations.

The standard enthalpy of formation is an important predictor of decomposition temperature for the decomposition reaction with its associated standard thermodynamic parameters. For a complex hydride, when the material is being heated, the effect of standard entropy starts dominating the standard enthalpy and at the decomposition temperature and constant pressure the standard Gibbs energy is zero. As during heating the entropy change of solid materials is very small compared to the gas, we can consider that the entropy change during the decomposition reaction is primarily due to H_2 evolution. Now at standard pressure and temperature for the most simple metal hydride, $\Delta S \approx \Delta S(H_2) = 130.7$ J/mol K (Ref. 17) which suggests that, for a simple hydride, the enthalpy of decomposition at room temperature (300 K) and 1 bar pressure is about 39 kJ/mol of H_2. For complex metal hydride materials it has been suggested that if the enthalpy of reaction is between 30 and 60 kJ/mol of H_2,[18] we can expect the complex metal hydride to be reversible for hydrogen storage.

We extended our theoretical calculations to identify the most favorable dehydrogenation reaction for $Zn(BH_4)_2$ by calculating the reaction enthalpies of different decomposition reactions. We expect that upon heating, $Zn(BH_4)_2$ releases hydrogen according to the following reaction during decomposition:

$$Zn(BH_4)_2 \rightarrow Zn + 2B + 4H_2(g) \tag{1a}$$

Other possible different decomposition reactions are given in Eqs. (1b)–(1e). Formation reactions for the decomposition products are given in Eqs. (2) and (3). Formation enthalpy is one good way to establish whether theoretically predicted phases are likely to be stable. Such results are also expected to guide us to the discovery of convenient synthesis routes:

$$Zn(BH_4)_2 \rightarrow Zn + B_2H_6 + H_2, \tag{1b}$$

$$Zn(BH_4)_2 \rightarrow ZnH_2 + 2B + 3H_2, \tag{1c}$$

$$Zn(BH_4)_2 \rightarrow \frac{1}{2}ZnH_2 + \frac{1}{2}Zn + 2B + \frac{7}{2}H_2, \tag{1d}$$

$$Zn(BH_4)_2 \rightarrow ZnH_2 + B_2H_6, \tag{1e}$$

$$2B + 3H_2 \rightarrow B_2H_6, \tag{2}$$

$$Zn + H_2 \rightarrow ZnH_2. \tag{3}$$

II. COMPUTATIONAL METHODS

A. *Ab initio*

First-principle calculations were performed on $Zn(BH_4)_2$ using DFT within the local density approximation[19] (LDA) and projected augmented wave[20,21] (PAW) method utilizing a plane wave basis set to calculate the total energies, as implemented in the Vienna *Ab initio* Simulation Package (VASP).[22–24] A $5\times5\times5$ Monkhorst-Pack[25] **k**-point mesh was used for sampling the Brillouin zone. A kinetic energy cutoff of 312 eV was used for $Zn(BH_4)_2$ for the plane wave basis set. For Zn, B, H_2, and B_2H_6, the same kinetic energy cutoff

TABLE II. The enthalpy of formation (in kJ/mol of H_2) of $Zn(BH_4)_2$ from DFT for structures based on a similar chemical formula unit complex.

Model	Z	Space group (number)	Type of unit cell	ΔH_{form} (0 K) kJ/mol H_2
$Ca(AlH_4)_2$	8	$Pbca(61)$ (Ref. 32)	Orthorhombic	−74.31
	2	$P2_1/c(14)$ (Ref. 33)	Monoclinic	14.10
	3	P-$62m(189)$ (Ref. 33)	Hexagonal	−6.36
	9	P-3(147) (Ref. 33)	Trigonal	−68.83
$Mg(AlH_4)_2$	1	P-$3m1(164)$ (Ref. 34)	Trigonal	5.27
$Mg(BH_4)_2$	2	$P2/c(13)$ (Ref. 5)	Monoclinic	−16.63
	2	$Pmc2_1(26)$ (Ref. 35)	Orthorhombic	−76.91
$Zn(BH_4)_2$	2	P-1(2) (Ref. 36)	Triclinic	−16.73
$Be(BH_4)_2$	16	$I4_1cd(110)$ (Ref. 37)	Tetragonal	−75.85
$Ca(BH_4)_2$	8	$Fddd(70)$ (Ref. 2)	Orthorhombic	−62.98

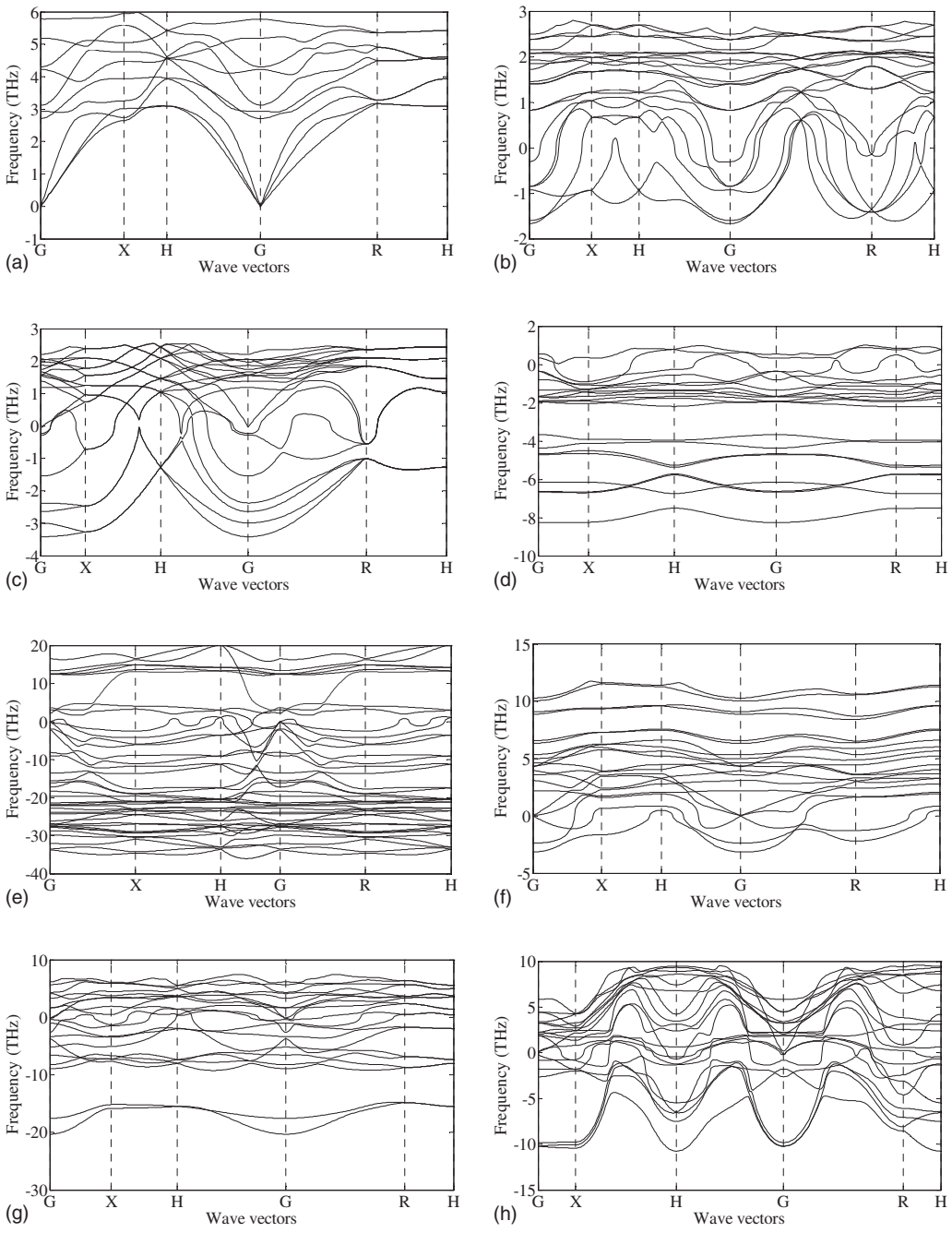

FIG. 1. (a)–(h) Phonon dispersion relations of the $Pmc2_1$, $I4_1cd$, $Pbca$, P-3, $Fddd$, P-1, $P2/c$, and P-62m space group structures of $Zn(BH_4)_2$. Coordinates of high-symmetry points are $\Gamma(0,0,0) \cong G(0,0,0)$, $X(1/2,0,0)$, $H(1/2,0,1/2)$, $R(1/2,1/2,1/2)$.

values as for $Zn(BH_4)_2$ were utilized, in the self-consistent total energy (Table I) calculations. This allows for the maximum cancellation of errors in the reaction enthalpy evaluation, which are calculated as small energy differences between reactants and products (Table II). The criterion for self-consistency in the electronic structure determination was that two consecutive total energies differed by less than 0.001 meV. The atomic positions and the lattice parameters, including the unit cell volume, were optimized by minimizing the forces and stresses until the residual forces between the atoms were within 1.0 meV/Å.

B. Direct method lattice dynamics

DFT is a nonempirical parameter method whose applications and predictive ability in different fields are known for some time. Combination of DFT with different techniques such as linear response method[38,39] or direct methods[16,40,41] allows us to evaluate phonon dispersion curves without empirical parameters. Parlinski *et al.*[42,43] developed the direct method where the forces are calculated via the Hellmann-Feynman theorem using DFT-derived total energies, assuming a finite range of interaction. The phonon spectra are then

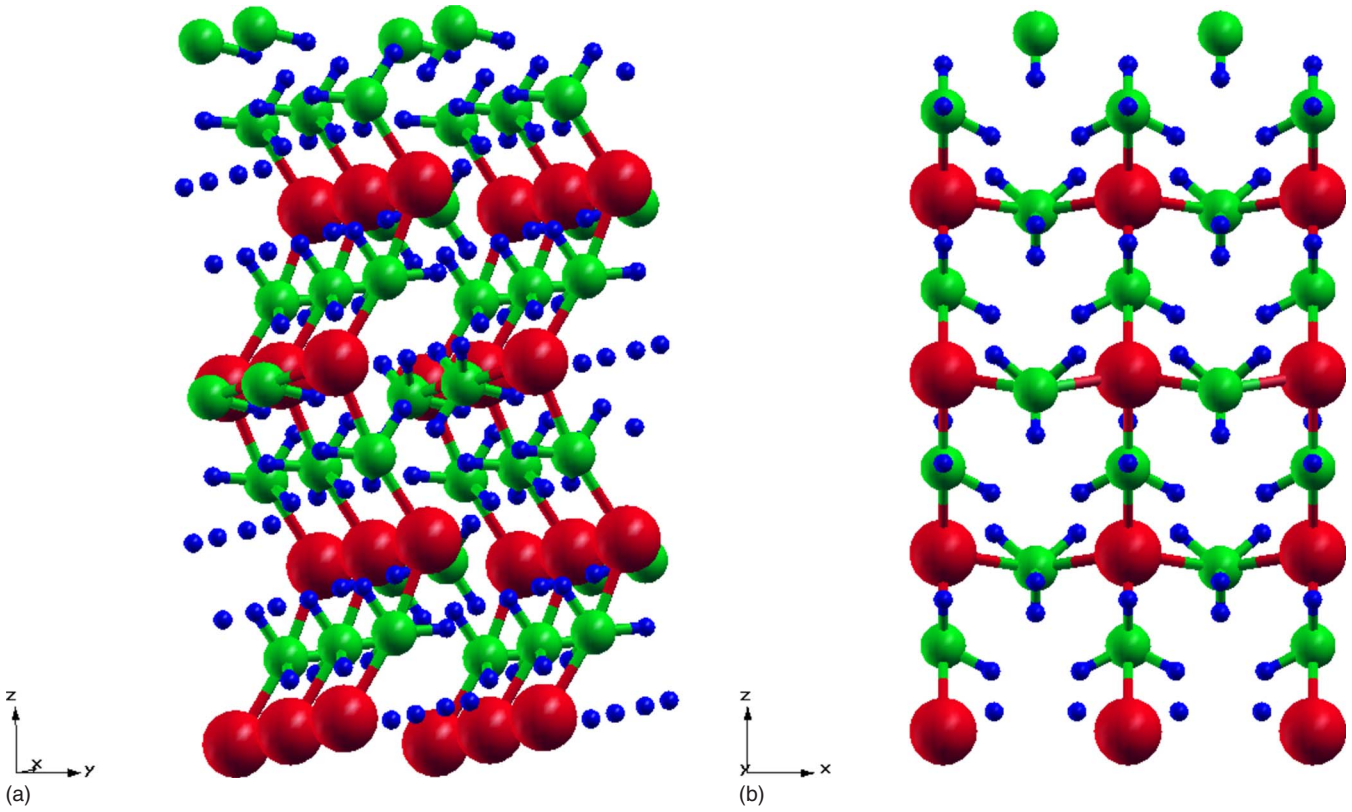

FIG. 2. (Color online) Orthorhombic structure of space group $Pmc2_1$ (No. 26) of $Zn(BH_4)_2$. (a) Proposed three-dimensional crystal structure and (b) projected structure along [010] plane. (Red: Zn, blue: H, and green: B atom).

derived using Newton's equation of motion in the lattice dynamics calculations.

The PHONON code,[44] based on the harmonic approximation, as implemented within MOLEKEL was used to calculate the phonon spectra. Based on the optimized crystal structure, a supercell consisting of a large number of atoms depending on the type of unit cell was generated from the conventional cell. The interaction range is confined to the interior of the extended supercell and the force constants at and beyond this extended supercell can be neglected. The asymmetric atoms were displaced by +/−0.02 Å. The dynamical matrix was obtained from the forces calculated via the Hellmann-Feynman theorem. This size of the supercell gives "exact" phonon frequencies at Γ, *X*, *H*, *R* Brillouin zone points in the dispersion curves.

III. RESULTS and DISCUSSION

$Zn(BH_4)_2$ is a potential candidate for hydrogen storage but very little is known about the thermodynamics of this material. We expect that upon heating, $Zn(BH_4)_2$ releases hydrogen according to reaction (1a) during decomposition. We calculated the enthalpy of reaction considering Eq. (1a) and based on the total energy calculation by combined DFT and direct method lattice dynamics using the following basic equation:

$$\Delta H = \sum_{\text{products}} E - \sum_{\text{reactants}} E. \tag{4}$$

The total energies of $Zn(BH_4)_2$, Zn, B, and H_2 were calculated by DFT to evaluate the enthalpy changes for reactions given above based on the following structures: different complex models listed in Table II for $Zn(BH_4)_2$, hcp for Zn ($P63/mmc$), trigonal for B (R-$3m$), and monoclinic for B_2H_6($P2_1/n$). We performed dimer calculations to determine the optimum binding energy for H_2 molecule, for which we used the constant velocity MD simulation method in VASP. In these calculations, the interionic distance was increased by 0.01 Å per time step of 1 fs staring from 0.65 Å and ending at 0.88 Å. All the structures were optimized during the total energy calculations. The calculated ground-state energies for each element are given in Table I. The following sections discuss the stable crystal structures, electronic structure, and finite temperature reaction enthalpy.

A. Crystal structure

The structure of zinc borohydride with the lowest enthalpy of formation was found to be of the $Mg(BH_4)_2$ type which has an orthorhombic structure in the space group of $Pmc2_1$ (No. 26). No literature studies are available for the crystal structure of $Zn(BH_4)_2$ except a recent one by Nakamori *et al.*[5] They have found that the crystal structure of $Zn(BH_4)_2$ is triclinic of space group P-1 (No. 2). They considered effective ionic radius of a $[BH_4]^-$ anion as 2.03 Å (Ref. 45) which is close to the ionic radii of Br^- 1.96 Å and I^- 2.20 Å. In DFT calculations, they considered structures of MX_2 (X=Cl, Br, and I; M=Mg, Zn, Hg, and Cd) for $Zn(BH_4)_2$ to find the most stable crystal structure, as an ionic bonding exists between Zn^{++} cations and $[BH_4]^-$ anions in $Zn(BH_4)_2$. Most of the commonly known complex hydrogen

storage materials which have the same formula unit as $Zn(BH_4)_2$ are given in Table II. We started our calculations for the $Zn(BH_4)_2$ from these known complex models and included the zinc borohydride structure established by Nakamori *et al.*[5] We optimized the atomic positions and cell parameters for the $Zn(BH_4)_2$ for each basis model and finally optimized the cell volume against the total energy. After that we calculated the enthalpy of formation using Eq. (4) for each model. Results from these calculations are shown in Table II. Negative enthalpy of formation is indicative of a thermodynamically stable structure.

In our calculations, we found that the stable structures are $Pmc2_1$, $I4_1cd$, $Pbca$, P-3, $Fddd$, P-1, $P2/c$, and P-62m. The highest negative enthalpy of formation (−76.91 kJ/mol of H_2) for $Zn(BH_4)_2$ was found for the space group $Pmc2_1$ [i.e., $Mg(BH_4)_2$ model]. Hence, we considered it to be the most stable structure of $Zn(BH_4)_2$ at 0 K. We found that the enthalpy of formation at 0 K for the P-1 space group to be −16.73 kJ/mol of H_2 without zero point energy (ZPE) corrections, which suggests this space group is not the most stable structure.

To establish finite temperature structural stability, we calculated the phonon spectra by the direct force constant lattice dynamics technique. The phonon spectra are shown in Fig. 1(a)–1(h): $Pmc2_1$, $I4_1cd$, $Pbca$, P-3, $Fddd$, P-1, $P2/c$, and P-62m space groups. We did not perform lattice dynamics calculations for space groups having positive enthalpy of formation without ZPE corrections as they are thermodynamically unstable. It can be seen from these dispersion curves that non-negative frequency distribution is present only for the $Pmc2_1$ space group. This suggests that $Pmc2_1$ space group (orthorhombic structure) is the stable structure for $Zn(BH_4)_2$ at finite temperatures. Only for this stable structure can acoustic and optical phonons be seen clearly in the dispersion curve.

The highest soft phonon mode for space group P-1 was found to be i3.75 THz which suggests that the crystal for this phase group is unstable. This finding contradicts the results of Nakamori *et al.*[5] Their not incorporating ZPE corrections and utilization of ultrasoft pseudopotentials (versus our more accurate PAW potentials) are possible reasons for this discrepancy. The PAW potentials give better accuracy for 3-d metal hydrides.[46] It is observed that for the structure with the most negative formation enthalpy, the soft phonon modes vanish. The $I4_1cd$, $Pbca$, P-3, $Fddd$, $P2/c$, and P-62m space groups showed the biggest soft modes of i1.667, i3.415, i8.75, i36.063, i20.25, and i12.25 THz, respectively, along different high symmetry directions.

The minimum total energy for $Zn(BH_4)_2$ is −44.595 eV/mol at a unit cell volume of 150.82 Å^3 (considering the $Pmc2_1$ to be the stable structure at finite temperatures). The optimized lattice parameters and atomic positions are given in Table III. Figure 2 shows the optimized orthorhombic ($Pmc2_1$) crystal structure. Our calculations showed nearly tetrahedral shape of the BH_4 complex with B-H bond lengths $d_{B\text{-}H}$=1.20–1.25 Å and H-B-H bond angles $\theta_{H\text{-}B\text{-}H}$=104.16–120°.Calculations of the phonon density of states (Fig. 3) allowed us to determine finite temperature thermodynamic properties. The results are described in detail in a subsequent section.

TABLE III. Optimized crystal structure of $Zn(BH_4)_2$. The space group is $Pmc2_1$ (No. 26) with lattice parameters a=4.118 Å, b=4.864 Å, c=7.916 Å. All the atomic positions are given by Wyckoff letter and the number of formula units in the unit cell Z=2.

Element	Wyckoff letter	X	Y	Z
Zn	2a	0.00000	0.28459	0.00890
B1	2b	0.50000	−0.06481	0.47060
B2	2a	0.00000	−0.46194	0.24842
H1	2b	0.50000	−0.30735	0.42745
H2	4c	0.27449	−0.00500	−0.42983
H3	2a	0.00000	0.39706	0.37973
H4	2a	0.00000	0.21066	−0.24017
H5	4c	0.25820	−0.48360	−0.32151
H6	2b	0.50000	0.08396	0.34880

In the phonon density of states, the phonon frequencies are classified into three groups. From the analysis of the eigenvectors, we found eigenmodes in the regions 25.75–39.75 THz and 65.75–76.75 THz which originate from internal B-H bending, and stretching vibrations in the $[BH_4]^-$ complex anion, respectively. These results compare well with the experimental solid state Fourier transform infrared spectroscopy analysis data (33.84 THz for B-H bending and 73.66 THz for B-H stretching).[7] As can be seen from Fig. 3, the librational frequencies (<22.25 THz) that originate from the displacement of Zn^{++} and $[BH_4]^-$, are lower than the B-H bending and stretching modes of $[BH_4]^-$.

B. Electronic structure

The local and total electronic density of states (DOS) were calculated for the finite temperature stable crystal structure of $Zn(BH_4)_2$, i.e., $Pmc2_1$, and are shown in Figs. 4 and 5. From these figures, it can be seen that $Zn(BH_4)_2$ is an insulating material with a fundamental band gap of 3.529 eV. For $Mg(AlH_4)_2$ quasiparticle GW corrections to DFT calculations give the actual excited state band gap of 6.5 eV,[29] which is 2.4 eV higher than DFT-calculated band gap of 4.1 eV.[34] Hence, we expect our calculated band gap of 3.529 eV to also be an underestimation. From the total density of states plot (Fig. 4), it can be observed that there are three main

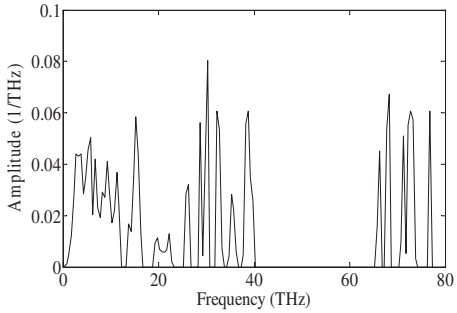

FIG. 3. Total density of phonon states $g(w)$ of $Zn(BH_4)_2$ in $Pmc2_1$ symmetry. Total phonon density of states is normalized as $\int g(w)dw=1$.

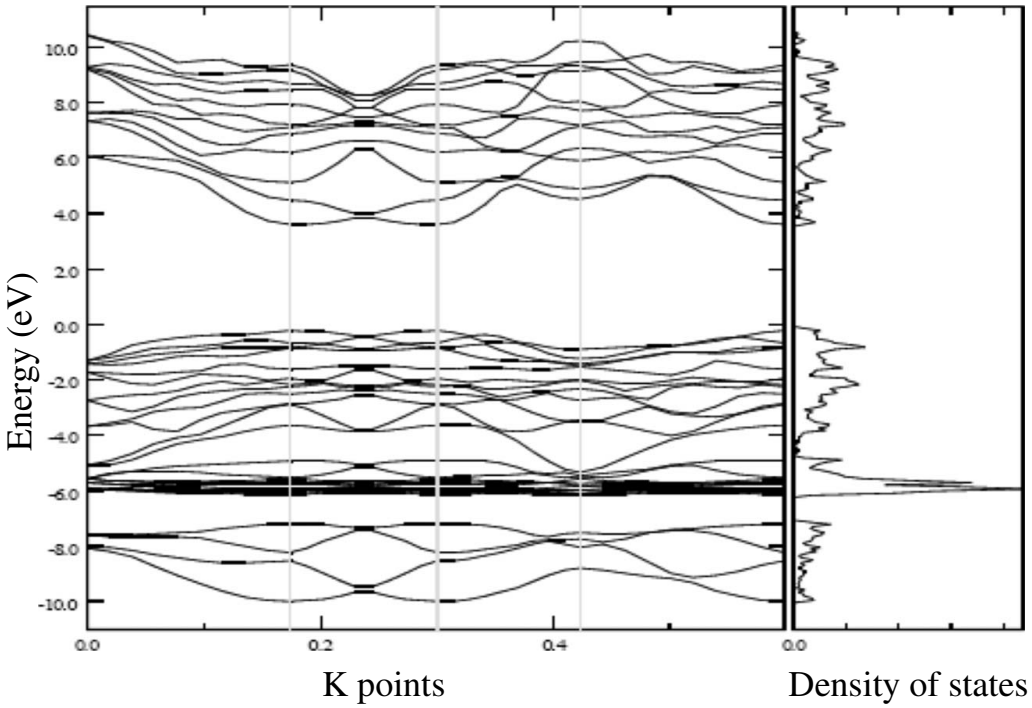

FIG. 4. DFT/LDA electronic band structure and total density of states (DOS) of $Zn(BH_4)_2$ relative to Fermi level.

valence bands and one conduction band. From the partial DOS plot (Fig. 5), it can be seen that the lowest valence band is dominated by B 2*s* electrons and H 1*s* electrons with negligible contribution from Zn. The middle part of the valence band is mainly dominated by Zn 3*d* electrons. The upper valence band is occupied by B 2*p* electrons and H 1*s* electrons, with a small contribution from Zn 3*d* electrons. The valence band is dominated by B 2*s* and H 1*s* electrons that make a strong B-H bond. The conduction band is primarily dominated by B 2*p* electrons and to a lesser extent B 2*s* and Zn 4*s* electrons. Although H *s* electrons are prominent in the valence band small states are also found in the conduction

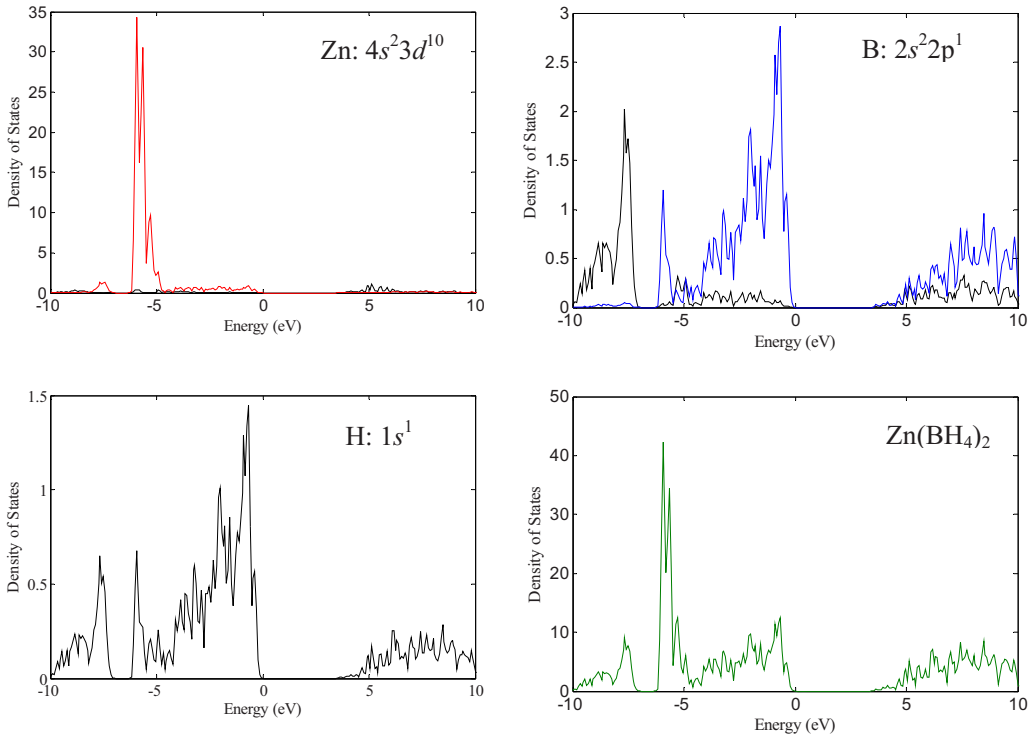

FIG. 5. (Color online) DFT/LDA electronic local/total density of state (DOS) relative to Fermi level for the most stable space group $Pmc2_1$ (No. 26) is orthorhombic structure (black line for *s*, blue line for *p*, and red line for *d* orbital).

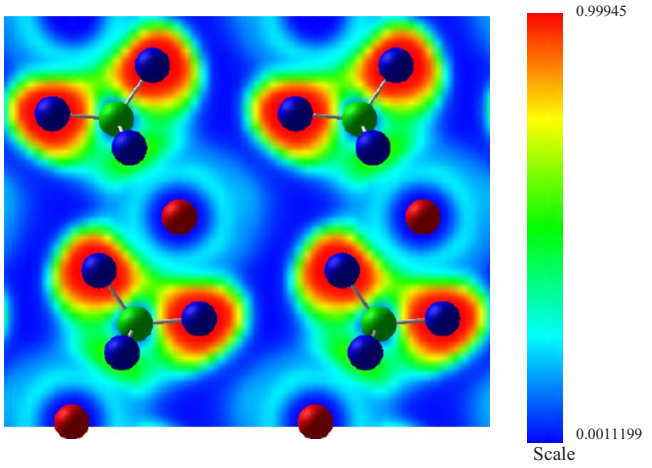

FIG. 6. (Color online) Electron localization function (ELF) of $Zn(BH_4)_2$ (100 plane) (Red: Zn, blue: H, and green: B).

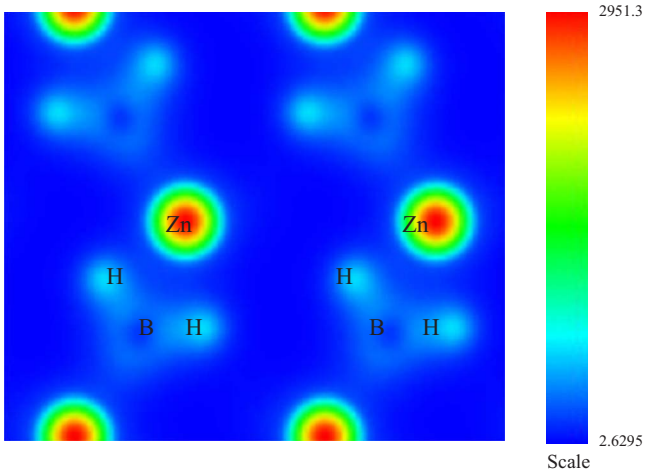

FIG. 7. (Color online) Charge density of $Zn(BH_4)_2$ (100 plane).

band, which may indicate charge transfer to H atoms.

The overall features of the DOS and PDOS, are different from those of $LiBH_4$,[1] $NaBH_4$,[45] KBH_4,[45] and $Mg(BH_4)_2$.[5] The main difference is that the valence band has three parts for $Zn(BH_4)_2$ whereas the above mentioned borohydrides have two major parts in the valence band. This may be due to the presence of *d* electrons from the Zn atom. However, further investigations are required before providing more specific interpretations.

The electron localization function[47,48] (ELF) and charge density for the $Zn(BH_4)_2$ (100) plane were calculated for the space group $Pmc2_1$ to study the bonding between the atoms. ELF is associated with the probability density of finding two electrons in the same spin-state close to each other. It is a position-dependent function which varies between 0 and 1. An ELF value of 0.5 means a gas-electron-like probability. The ELF calculated here (Fig. 6) shows strong and large attractors around the H atoms. Hydrogen has no core attractor, thus this indicates either a shared-electron or a closed-shell bond. The very low ELF value on the B sites indicates delocalized electrons, while a spherical shell attractor is seen around Zn. The very low ELF value between Zn and $[BH_4]^-$ complex indicates the low ionic bond. Whereas, a very high value of ELF within the $[BH_4]^-$ complex indicates ionocovalent bonding. The plotted charge density (Fig. 7) shows large densities centered around Zn which is segregated from B and H atoms. Some density is found around the H atom; however, it is significantly lower than around the Zn atom. Almost no charge density is seen around B. This also suggests that electrons are transferred to the H atom mostly from the B atom resulting in a strong B-H bond in the $[BH_4]^-$ complex with less polar bonding between the Zn and H atoms.

C. Finite temperature reaction enthalpy

In the thermodynamic expression for the finite temperature enthalpy

$$H(T) = E(T) + PV, \tag{5a}$$

$E(T)$ is the total internal energy which includes not only energies from DFT and ZPE (at 0 K) but also contributions from rotational, translational, and vibrational (excluding ZPE) energies given in Eq. (5b). We assumed that other rotational and translational energies are important for the gaseous phase only:

$$E = E_{\mathrm{DFT}}(0\ \mathrm{K}) + E_{\mathrm{ZPE}}(0\ \mathrm{K}) + E_{\mathrm{vib}}(T) + E_{\mathrm{rot}}(T) + E_{\mathrm{tran}}(T). \tag{5b}$$

The enthalpy of formation is now given by Eq. (6a), as a sum of the absolute zero temperature part and the finite temperature part. The first part [Eq. (6b)] includes the ground-state energy and also the zero point vibrational energy which is independent of temperature. On the other hand, the finite temperature part [Eq. (6c)] includes all the energies which are dependent on temperature, and is calculated using statistical mechanical theory:

$$\Delta H_{\mathrm{form}}(T) = \Delta H^0(0\ \mathrm{K}) + \delta\Delta H(T), \tag{6a}$$

where

$$\Delta H^0(0\ \mathrm{K}) = \Delta E_{\mathrm{DFT}}(0\ \mathrm{K}) + \Delta E_{\mathrm{ZPE}}(0\ \mathrm{K}), \tag{6b}$$

$$\Delta E_{\mathrm{DFT}}(0\ \mathrm{K}) = \sum_{\mathrm{products}} E_{\mathrm{DFT}}(0\ \mathrm{K}) - \sum_{\mathrm{reactants}} E_{\mathrm{DFT}}(0\ \mathrm{K}), \tag{6b1}$$

$$\Delta E_{\mathrm{ZPE}}(0\ \mathrm{K}) = \sum_{\mathrm{products}} E_{\mathrm{ZPE}}(0\ \mathrm{K}) - \sum_{\mathrm{reactants}} E_{\mathrm{ZPE}}(0\ \mathrm{K}), \tag{6b2}$$

and

$$\delta\Delta H(T) = \Delta E_{\mathrm{vib}}(T) + \Delta E^g_{\mathrm{rot}}(T) + \Delta E^g_{\mathrm{tran}}(T) + \Delta(PV), \tag{6c}$$

$$\Delta E_{\mathrm{vib}}(T) = \sum_{\mathrm{products}} E_{\mathrm{vib}}(T) - \sum_{\mathrm{reactants}} E_{\mathrm{vib}}(T), \tag{6c1}$$

$$\Delta E^g_{\mathrm{rot}}(T) = \sum_{\mathrm{products}} E^g_{\mathrm{rot}}(T) - \sum_{\mathrm{reactants}} E^g_{\mathrm{rot}}(T), \tag{6c2}$$

TABLE IV. Zero point and vibrational energies of $Zn(BH_4)_2$ and its primary elements.

Element/ compound	E_{ZPE} (kJ/unit formula) (literature)	E_{ZPE} (kJ/unit formula) (calculated)	E_{vib}(300 K) (kJ/unit formula) (includes ZPE)	E_{vib}(300 K) (kJ/unit formula) (actual)
Zn	1.0 (approx.) (Ref. 49)	1.077	7.176	6.099
α-B	12.5 (Ref. 50)	12.478	13.65	1.172
H_2	28.29 (Ref. 29), 27.08 (Ref. 51), 25.7 (Ref. 50)	28.12	≈28.12	≈0.0
B_2H_6	170.96 (Ref. 51)	163.367	173.473	10.106
$Zn(BH_4)_2$		206.539	225.404	18.811

$$\Delta E^g_{\text{tran}}(T) = \sum_{\text{products}} E^g_{\text{tran}}(T) - \sum_{\text{reactants}} E^g_{\text{tran}}(T). \quad (6c3)$$

For calculating $\delta\Delta H(T)$, as an example for the reaction given in Eq. (1a), we write [Eqs. (7)–(9)]

$$\delta\Delta H(T) = E^{Zn(BH_4)_2}_{\text{vib}}(T) - E^{Zn}_{\text{vib}}(T) - 2E^{B}_{\text{vib}}(T) - 4[E^{H_2}_{\text{vib}}(T) + E^{H_2}_{\text{tran}}(T) + E^{H_2}_{\text{rot}}(T) + PV], \quad (7)$$

$$\delta\Delta H(T) = E^{Zn(BH_4)_2}_{\text{vib}}(T) - E^{Zn}_{\text{vib}}(T) - 2E^{B}_{\text{vib}}(T) - 4\left[E^{H_2}_{\text{vib}}(T) + \frac{3}{2}k_BT + k_BT + k_BT\right], \quad (8)$$

$$\delta\Delta H(T) = E^{Zn(BH_4)_2}_{\text{vib}}(T) - E^{Zn}_{\text{vib}}(T) - 2E^{B}_{\text{vib}}(T) - 4\left[E^{H_2}_{\text{vib}}(T) + \frac{7}{2}k_BT\right]. \quad (9)$$

Equation (9) shows that we need to calculate the vibrational energy of the complex material $Zn(BH_4)_2$ and its elemental components to calculate the finite temperature reaction enthalpy. Vibrational energies in the above Eq. (9) were calculated by integrating the phonon density of states over the Brillion zone. The results for the E_{ZPE} and E_{vib} (without ZPE) for different elements and compounds are given in Table IV.

The enthalpy of formation of $Zn(BH_4)_2$ was found to be −76.91 kJ/mol of H_2 at 0 K [using Eq. (6b1)] without the zero point energy corrections and −59.90 kJ/mol of H_2 including ZPE [using Eqs. (6b) and (6b2)]. We also found that the finite temperature reaction enthalpy for the dehydrogenation reaction (1a) by using Eqs. (6a) and (9) was 66.003 kJ/mol H_2 at 300 K or 264.012 kJ/mol of $Zn(BH_4)_2$. The *ab initio* theoretical formation enthalpy value of ZnH_2 [reaction (3)] from zinc and molecular hydrogen varies from 6.464 to 31.57 kJ/mol ZnH_2.[52] As very little is known about ZnH_2, we calculated the formation enthalpy of the ZnH_2 using fluorite type structure and it was found to be 23.66 kJ/mol ZnH_2 at 0 K in our calculations for the dehydrogenation reactions (1c)–(1e). For reaction (2), we calculated the formation enthalpy of diborane. It was found to be 25.38 kJ/mol of B_2H_6 at 0 K including zero point energy whereas the experimental standard enthalpy of formation is 36.00 kJ/mol of B_2H_6.[53] We defined the standard enthalpy of reaction ΔH_{rxn} for the reaction (1b) as given below:

$$\Delta H_{rxn} = \Delta H^0_{\text{form}}(B_2H_6) - \Delta H^0_{\text{form}}[Zn(BH_4)_2]. \quad (10)$$

Similar expressions were used for other reactions. Using the standard formation enthalpies of $Zn(BH_4)_2$, B_2H_6, and ZnH_2 we found ΔH_{rxn} for the reactions (1b)–(1e) to be 300.012, 287.672, 284.440, and 323.672 kJ/mol of $Zn(BH_4)_2$, respectively. Although H_2 is released from the liquid phase, we have not included the heat of fusion for the dehydrogenation reaction enthalpy. So we can expect the enthalpy of formation values calculated to be overestimated. As the enthalpy of dehydrogenation of $Zn(BH_4)_2$ for the reaction (1a) is the lowest, this reaction may be expected to start first upon heating the complex borohydride. So this reaction can be predicted as the most favorable decomposition reaction. However, Jeon *et al.*[7] have found some evolution diborane experimentally, which indicates that reaction (1b) [36.00 kJ/mol higher enthalpy of dehydrogenation than reaction (1a)] also occurs at the same time. The exact quantification and identification of the decomposed gaseous components at the decomposition temperature of $Zn(BH_4)_2$ is beyond the scope of this work. The main objective of the work in this section was to find the thermodynamically most favorable decomposition reaction.

IV. CONCLUSIONS

In this work, we have predicted from theory the stability of the complex zinc borohydride structure. This required investigation of both the ground-state energy by DFT and the lattice vibration energy by direct method lattice dynamics. We have calculated the structural stability of $Zn(BH_4)_2$ at $T>0$ from structure-optimization calculations starting with ten different very similar formula units for $Zn(BH_4)_2$. These calculations establish $Pmc2_1$ symmetry to be a new thermodynamically most stable structure of $Zn(BH_4)_2$ at finite temperature. Our estimated value for the formation enthalpy of $Zn(BH_4)_2$ is −66.003 kJ/mol H_2 at 300 K which suggests that it should be possible to synthesize this phase. This finding suggests that the crystal structure is stable at room temperature and thus $Zn(BH_4)_2$ could be considered a potential candidate for hydrogen storage. The other thermodynamically stable structures in Table II which are $I4_1cd$, $Pbca$,

P-3, and *Fddd* symmetries, turn out to be unstable at finite temperatures with respect to lattice vibrations. From electronic structure calculations, ionic interaction between Zn and $[BH_4]^-$ and the strong ionocovalent B-H interaction within the $[BH_4]^-$ tetrahedral are revealed. Electronic density of states studies reveal that this phase has wide-band-gap of 3.529 eV which suggests that the $Zn(BH_4)_2$ is an insulator. Standard reaction enthalpy calculations reveal that decomposition to primary elements is the most favorable one. The findings of our work are in qualitative agreement with experimental results. Our study has given new insights into the thermodynamically most stable phase for the complex zinc borohydride. The methodology outlined in this work can be extended to studies on other complex hydrogen storage materials.

ACKNOWLEDGMENTS

We acknowledge the U.S. Department of Energy (Hydrogen Fuel Initiative Grant No. DE-FG36-04G014224) for funding. We also thank Academic Computing at the University of South Florida for providing computational resources.

*venkat@eng.usf.edu

[1] K. Miwa, N. Ohba, S.-i. Towata, Y. Nakamori, and S.-i. Orimo, Phys. Rev. B **69**, 245120 (2004).
[2] K. Miwa, M. Aoki, T. Noritake, N. Ohba, Y. Nakamori, S.-i. Towata, A. Züttel, and S.-i. Orimo, Phys. Rev. B **74**, 155122 (2006).
[3] A. Züttel, S. Rentsch, P. Fischer, P. Wenger, P. Sudan, Ph. Mauron, and Ch. Emmenegger, J. Alloys Compd. **356–357**, 515 (2003).
[4] Z. Łodziana and T. Vegge, Phys. Rev. Lett. **93**, 145501 (2004).
[5] Y. Nakamori, K. Miwa, A. Ninomiya, H. Li, N. Ohba, S.-i. Towata, A. Züttel, and S.-i. Orimo, Phys. Rev. B **74**, 045126 (2006).
[6] W. Grochala and P. P. Edwards, Chem. Rev. (Washington, D.C.) **104**, 1283 (2004).
[7] E. Jeon and Y. Cho, J. Alloys Compd. **422**, 273 (2006).
[8] J. Hafner, C. Wolverton, and G. Ceder, MRS Bull. **31**, 659 (2006).
[9] E. H. Majzoub, K. F. McCarty, and V. Ozolins, Phys. Rev. B **71**, 024118 (2005).
[10] J. F. Herbst and J. L. G. Hectro, Appl. Phys. Lett. **88**, 231904 (2006).
[11] T. Vegge, Phys. Chem. Chem. Phys. **8**, 4853 (2006).
[12] A. Marashdeh *et al.*, Chem. Phys. Lett. **426**, 180 (2006).
[13] J. Íñiguez, T. Yildirim, T. J. Udovic, M. Sulic, and C. M. Jensen, Phys. Rev. B **70**, 060101(R) (2004).
[14] N. A. Zarkevich and D. D. Johnson, Phys. Rev. Lett. **97**, 119601 (2006).
[15] P. Vajeeston *et al.*, Appl. Phys. Lett. **89**, 071906 (2006).
[16] K. Parlinski, Z.-Q. Li, and Y. Kawazoe, Phys. Rev. Lett. **78**, 4063 (1997).
[17] Q. Zeng, K. Su, L. Zhang, Y. Xu, L. Cheng, and X. Yan, J. Phys. Chem. Ref. Data **35**, 1385 (2006).
[18] S. V. Alapati, J. K. Johnson, and D. S. Sholl, J. Phys. Chem. B **110**, 8769 (2006).
[19] J. P. Perdew, J. A. Chevary, S. H. Vosko, K. A. Jackson, M. R. Pederson, D. J. Singh, and C. Fiolhais, Phys. Rev. B **46**, 6671 (1992).
[20] P. E. Blochl, Phys. Rev. B **50**, 17953 (1994).
[21] G. Kresse and D. Joubert, Phys. Rev. B **59**, 1758 (1999).
[22] G. Kresse and J. Furthmüller, Phys. Rev. B **54**, 11169 (1996).
[23] G. Kresse and J. Furthmüller, Comput. Mater. Sci. **6**, 15 (1996).
[24] G. Kresse and J. Hafner, Phys. Rev. B **47**, 558 (1993).
[25] H. J. Monkhorst and J. D. Pack, Phys. Rev. B **13**, 5188 (1976).
[26] http://www.mkmc.dk/crystal/194/Mg/Zn/main.html
[27] C. H. Park and D. J. Chadi, Phys. Rev. B **49**, 16467 (1994).
[28] http://www.webelements.com/webelements/properties/text/definitions/crystal-structure.html
[29] M. J. van Setten, G. A. de Wijs, V. A. Popa, and G. Brocks, Phys. Rev. B **72**, 073107 (2005).
[30] http://cst-www.nrl.navy.mil/lattice/struk.xmol/alphaB.pos
[31] D. L. V. K. Prasad, M. M. Balakrishnarajan, and E. D. Jemmis, Phys. Rev. B **72**, 195102 (2005).
[32] O. M. Løvvik, Phys. Rev. B **71**, 144111 (2005).
[33] C. Wolverton and V. Ozolins, Phys. Rev. B **75**, 064101 (2007).
[34] O. M. Løvvik and P. N. Molin, Phys. Rev. B **72**, 073201 (2005).
[35] P. Vajeeston, P. Ravindran, A. Kjekshus, and H. Fjellvåg, Appl. Phys. Lett. **89**, 071906 (2006).
[36] N. Kitajima, H. Shimanouchi, Y. Ono, and Y. Sasada, Bull. Chem. Soc. Jpn. **55**, 2064 (1982).
[37] D. S. Marynick and W. N. Lipscomb, Inorg. Chem. **11**, 820 (1972).
[38] S. Baroni, S. de Gironcoli, and P. Giannozzi, Phys. Rev. Lett. **65**, 84 (1990).
[39] S. Baroni, P. Giannozzi, and A. Testa, Phys. Rev. Lett. **58**, 1861 (1987).
[40] W. Frank, C. Elsässer, and M. Fähnle, Phys. Rev. Lett. **74**, 1791 (1995).
[41] S. Wei and M. Y. Chou, Phys. Rev. B **50**, 2221 (1994).
[42] K. Parlinski, J. Alloys Compd. **328**, 97 (2001).
[43] K. Parlinski and M. Parlinska-Wojtan, Phys. Rev. B **66**, 064307 (2002).
[44] K. Parlinski, software PHONON, 2005.
[45] C. W. F. T. Pistorius, Z. Phys. Chem., Neue Folge **88**, 253 (1974).
[46] http://cms.mpi.univie.ac.at/vasp-workshop/
[47] A. D. Becke and K. E. Edgecombe, J. Chem. Phys. **92**, 5397 (1990).
[48] B. Silvi and A. Savin, Nature (London) **371**, 683 (1994).
[49] G. Borelius, Phys. Scr. **18**, 9 (1978).
[50] D. J. Siegel, C. Wolverton, and V. Ozolins, Phys. Rev. B **75**, 014101 (2007).
[51] S.-W. Hu, Y. Wang, X.-Y. Wang, T.-W. Chu, and X.-Q. Liu, J. Phys. Chem. A **107**, 9974 (2003).
[52] T. M. Greene, W. Brown, L. Andrews, A. J. Downs, G. V. Chertihin, N. Runeberg, and P. Pyykkö, J. Phys. Chem. **99**, 792 (1995).
[53] http://en.wikipedia.org/wiki/Diborane